



Magnetic Resonance Imaging for Quality Evaluation of Fruits: a Review

R. K. Srivastava¹ · Sekhar Talluri¹ · Sk. Khasim Beebi¹ · B Rajesh Kumar²

Received: 15 December 2017 / Accepted: 9 April 2018 / Published online: 5 May 2018
© Springer Science+Business Media, LLC, part of Springer Nature 2018, corrected publication May/2018

Abstract

This article is a review of the magnetic resonance (MR)-based technologies that have been used for non-destructive quality assessment of fruits. The potential of these MR-based methods for commercial applications such as sorting or labelling is discussed. Although nuclear magnetic resonance (NMR) spectroscopy and magnetic resonance imaging (MRI) have been demonstrated to be quite effective for non-destructive characterization and quality evaluation of fruits, they have found only limited applications in current industrial and commercial applications. The limitations of the current MRI methodologies, and the technologies under development that have the potential to overcome these limitations, are also discussed. This review is limited to applications of MRI/NMR to non-invasive studies of fruits, with potential for industrial applications, and does not include applications of MRI/ NMR to vegetables, cereals and processed food items.

Keywords Magnetic resonance imaging · NMR spectroscopy · Fruit quality · Relaxation time · Quality assessment

Abbreviations

ANN	Artificial neural network	IR	Inversion recovery
CHESS	Chemical shift selective	MAE	Mean absolute error
CMOS	Complementary metal-oxide semiconductor	MRI	Magnetic resonance imaging
CPMG	Carr Purcell Meiboom Gill	MRIL	Magnetic resonance imaging logging
DC	Diffusion coefficient	MRSI	Magnetic resonance spectroscopic imaging
DHVT	Dimensional histogram variance thresholding	NIR	Near infrared
FLASH	Fast Low Angle Shot	NMR	Nuclear magnetic resonance
FOV	Field of view	PD	Proton density
Gx	Gradient magnitude in the x-direction	PGSE	Pulsed field gradient spin echo
Gy	Gradient magnitude in the y-direction	QA/QC	Quality assurance/quality control
Gz	Gradient magnitude in the z-direction	RF	Radio frequency
1H	Proton	RH	Relative humidity
		RWC	Relative water content
		SQUID	Superconducting quantum interference based detector
		SSC	Soluble solids content
		T ₁	Spin-lattice (longitudinal) relaxation time
		T ₂	Spin-spin (transverse) relaxation time
		(1/T ₂)	Spin-spin relaxation rate
		TE	Echo delay
		TR	Repetition time (time between repetitive application of pulse sequence)

Highlights

- Review of applications of MRI for non-destructive characterization of fruits
- Limitations of current/reported MRI technology for fruit quality assessment
- Discussion of MRI technology under development for fruit quality assessment

✉ R. K. Srivastava
rajeshksrivastava73@yahoo.co.in

¹ Department of Biotechnology, GIT, GITAM University, Rushikonda, Visakhapatnam, AP 530045, India

² Department of Electronics and Instrumentation Engineering, GIT, GITAM University, Rushikonda, Visakhapatnam, AP 530045, India

Introduction

Numerous non-invasive methods have been developed for quality evaluation and sorting of agricultural products such

as fruits (Zion et al. 1995b; Abbott 1999). These methods are based on measurement of properties such as density, firmness, surface texture, vibration characteristics, X-ray and gamma ray transmission, optical reflectance and transmission, electrical properties, magnetic properties and magnetic resonance (MR) (Chen et al. 1989; Zou and Zhao 2015). Non-destructive methods for quality assessment and sorting of fruits have been reviewed earlier (Chen and Sun 1991; Butz et al. 2005; Arendse et al. 2018). The objective of present review is to describe applications of MR based methods for fruit quality assessment or control, the limitations of the existing MR based methods, and the novel MR-based technologies that are being developed to overcome the limitations.

Magnetic resonance-based techniques such as NMR spectroscopy (Bloch et al. 1946; Bloembergen et al. 1948), MRI (Lauterbur 1973; Kumar et al. 1975) and MR spectroscopic imaging (MRSI) are completely non-invasive and can provide detailed information regarding the internal structure of fruits (Shaw and Elsken 1956; Gunasekaran 2000).

MR spectral attributes such as intensity, chemical shift, relaxation time, line-width and line-shape can be measured in a spatially resolved manner. Such information can be utilized for quality assessment, prediction of the stage of maturity of the fruit and shelf life (Clark et al. 1997), and to estimate the optimum time for consumption. The reliability of application of MRI in medical diagnostics (Brant and de Lange 2012), plant science (Faust et al. 2010) and food science (Schmidt et al. 1996; Farhat et al. 2007) is evidence of its potential for such applications. However, some MR techniques, such as MR microscopy (Callaghan et al. 1994), that have found extensive application in plant and food science (Sarafis et al. 1990) are of limited use in QA/QC applications, because the requirements of magnetic field strength, homogeneity and magnetic field gradient strength for MR-microscopy are higher than those that are used in routine medical MRI. The primary challenges in large scale application of MR technologies for commercial and industrial applications related to food quality assessment are the high cost, large size and weight of the magnets, interference from external electromagnetic fields and metallic materials, high throughput requirements and the susceptibility to mechanical vibrations and other motion based artifacts.

Magnetic Resonance-Based Sensors for Quality Assessment of Fruits

The physical principles and properties of the measurable attributes of relevance to MR phenomena (MRI/NMR) have been described and reviewed earlier (Brown et al. 2014). The molecular constituents of fruits contain MR active nuclei and these nuclei can be used as sensors of the internal structure, texture, taste and other indicators of fruit quality (Colnago et al. 2014). The following sections summarize the MR attributes that have been used, or have the potential, for quality assessment of fruits.

Measurable Attributes of MR-Based Methods

Proton Density

Proton is the preferred nucleus for most imaging studies of fruits due to its high abundance, high magnetogyric ratio and sensitivity (Galed et al. 2004). MRI experiments designed to map the proton density (either 2D or 3D) provide detailed information regarding the internal structure of objects such as fruits. Differences in the patterns of proton density can be used to identify physical defects such as injury and drying, as well as biological defects such as drying, aging (rotting) and presence of microbial infection (Clark et al. 1997).

Relaxation Time

Bloembergen et al. have discussed the longitudinal relaxation time T_1 and it is the time constant that characterizes the time required for the net spin magnetization to return to the equilibrium state after a perturbation from the equilibrium state (Bloembergen et al. 1948). It depends on the rotational correlation time of the nucleus, its interactions with neighboring nuclei and on the magnetic field (Solomon 1955). The rotational correlation time depends on the size and shape of the molecule, its internal degrees of freedom as well as on the viscosity and temperature of the surrounding solvent. Therefore, T_1 is a sensitive measure of motional freedom of the nucleus under study. Variation of T_1 can be used as a contrast enhancement mechanism in MRI (Bydder and Young 1985). The viscosity of water varies substantially depending upon the tissue type. Hence, an MRI map showing the variation of T_1 as a function of position can be used, in some cases, to identify defects that may be difficult to detect in proton density mapping (Kirtil et al. 2017). The sweetness of many fruits depends upon the total soluble sugar content, and the soluble sugar content alters the viscosity of the solution, and this alters the T_1 . Hence, measurements of T_1 have the potential for non-invasive assessment of sweetness, which is one of the factors used to judge the quality and level of maturity of fruits (Andaur et al. 2004).

The transverse relaxation time (T_2) is the time constant that characterizes the time required for the magnitude of the net transverse spin magnetization vector to attain its equilibrium value of zero (Keeler 2013). T_2 depends on the interactions of the nuclei with other nuclei, on the magnetic field and magnetic field inhomogeneity, and the rotational correlation time (Solomon 1955; Redfield 1957). However, T_2 and T_1 have different dependence on these factors. Therefore, T_2 weighted MR images can provide information that is complimentary to T_1 weighted and density weighted MR images and this information can be utilized for monitoring the ripening stage and quality of fruits (Marcone et al. 2013; Zhang and McCarthy 2013). For high throughput applications of MRI on fruits, T_2

measurements are technologically more challenging, because of the strong dependence of T_2 on magnetic field homogeneity which places stringent requirements on the quality of the magnet and the homogeneity of the magnetic field used for such applications. Although such stringent requirements are routinely satisfied in MRI instruments used for research and medical diagnostic applications as well as for NMR spectrometers used for biological applications, it contributes significantly to the cost of the instrument which is a much more significant issue in commercial applications dealing with the quality assessment of fruits.

Chemical Shifts

The chemical shift (Dickinson 1950; Proctor and Yu 1950) is the ratio of the change in the resonance frequency of the nucleus of interest to the resonance frequency of a reference nucleus measured at the same magnetic field (Ramsey 1950). The chemical shifts can provide information regarding the chemical constitution (Sarafis et al. 1990) and hence are sensitive indicators of quality and maturity of fruits as the presence (and quantity) of specific chemicals can act as markers (Tse et al. 1996). Fat and water have sufficiently distinct chemical shifts to permit assessment of the fat or oil and water content of fruits, which can be a significant factor with regard to utility in some cases (Pope et al. 1991). Chemical Shift Imaging (CSI) may be used for spectral resolution enhancement (Sersa and Macura 2007). The potential of CSI for studies of bruises in apples and plums has been investigated (Cheng et al. 2008). Voxel-selective point resolved spectroscopy (PRESS) was used for endosperm vacuole composition characterization in intact pea seeds and CSI was used to map metabolite distribution during development (Melkus et al. 2009). CSI has been used for lipid-imaging in several plants (Munz et al. 2016). Magnetic resonance spectroscopic imaging (MRSI) is technically more demanding than MRI (Bottomley and Griffiths 2016). Although this may be a limitation for commercial applications involving high throughput MRSI of fruits, a platform for imaging and quantifying oil storage in tobacco seeds with a throughput of 2.6 min/seed has been demonstrated (Fuchs et al. 2013).

Heteronuclei

^1H is the preferred nucleus for MRI studies due to the high natural abundance in fruits and the high magnetogyric ratio of ^1H . Other common nuclei that occur in fruits, ^{12}C , ^{14}N and ^{16}O cannot be observed by MRI. However, the less abundant isotopes, ^{13}C , ^{15}N and ^{17}O can be studied by magnetic resonance. In situ studies of lipid components have been carried out using high-resolution solid-state ^{13}C NMR and pulsed field gradient NMR to characterize the liquid and solid

domains of plant seeds (Gromova et al. 2016). ^1H - ^{13}C cyclic J cross-polarization PGSE was introduced for selective observation of oil component in a combined imaging and diffusion experiment. The spatial dimensions of oil droplets in xanthum gum water emulsions could be determined with this technique (McDonald et al. 1999). ^1H detected ^{13}C MRI has been utilized for studies of labeled sucrose transport in plants (Heidenreich et al. 2008).

Diffusion Constants

The diffusion constant of water within firm tissues is substantially different from that in liquid water or necrotic tissue. Spin-echo based pulse sequences (Carr and Purcell 1954), that are sensitive to diffusion, can be incorporated into standard MR imaging pulse sequences to obtain diffusion weighted images (Callaghan et al. 1994). Diffusion weighted MRI can provide information on the spatial dependence of diffusion constants and this information can be used to study fruit maturation and ripening (Ishida et al. 1997; Dean et al. 2014), or degradation effects such as internal browning (Defraeye et al. 2013).

NMR/MRI Hardware

NMR Hardware for Static MR/NMR Spectroscopy

Conventional MR/NMR Spectrometers

The basic components of the conventional MRI/NMR spectrometers are: magnet, probe, RF synthesizer, A/D converters, amplifiers, shielded magnetic field gradients and control electronics (Fukushima and Roeder 1993). The essential difference between the hardware for an NMR spectrometer from that of an MR Imager is that the MR Imagers have a magnet with a wider bore and magnetic field homogeneity is maintained over a larger volume to permit imaging of larger objects and are equipped with triple-axis magnetic field gradients of higher strength than those of conventional NMR spectrometers (Bottomley 1982). High resolution NMR spectrometers and MR imagers use superconducting magnets. These superconducting magnets require liquid Helium and Nitrogen refilling. The newer magnet designs based on cryogen recovery minimize the cryogen loss. Although cryogen recovery substantially reduces the maintenance costs and overheads, it increases the initial cost and size of the instrument. The majority of magnets used for MR applications in industry utilize permanent magnets which do not require regular maintenance. The permanent magnets are usually made from NdFeB and/or SmCo and consist of two poles (Mitchell et al. 2014). A connector made

of soft iron is often used to stabilize and enhance the magnetic field in a small volume inside the magnet where the sample of interest is placed. Although the magnetic field obtainable from the permanent magnets is smaller than that for superconducting magnets, permanent magnets are preferred for industrial QA/QC applications because of lower maintenance cost and lower sensitivity to environmental variables (Danieli et al. 2010).

Portable and Miniature MRI/NMR Spectrometers

Small, dedicated MRI instruments have been developed for applications in food science and agriculture (Constantinesco et al. 1998; Koizumi et al. 2008). Further attempts at miniaturization are in progress. Substantial progress has been achieved in miniaturization of the electronic components. Integration of the probe as well as micro fluidics for sample input/output into a single board that includes all the necessary RF electronics for NMR spectroscopy has been demonstrated (Sun et al. 2011). A portable NMR sensor has been developed for measurement of dynamic changes in fruits (Windt and Blumler 2015).

With the current permanent magnet technology, for a fixed mass of magnet, the usable sample volume decreases with increase of homogeneous magnetic field strength (Blumich 2016). Therefore, desktop and portable MRI/NMR spectrometers have been most successful in applications that are feasible with low or intermediate magnetic fields on relatively small objects (Danieli et al. 2010). Alternate methods for obtaining MR data in inhomogeneous magnetic fields, such as stray field imaging (Chudek and Hunter 2002), are being developed for imaging of objects that are larger than the size of magnets used for obtaining MRI data (see Section 7).

Data Acquisition

The number, amplitude, shape, duration, frequency, phase and timing of RF pulses and the number, amplitude, shape, duration and timing of pulsed magnetic field gradients, can be controlled in NMR and MRI experiments (Talluri and Scheraga 1990; Talluri and Wagner 1996). Pulse sequences are available for obtaining proton (water) density weighted, T_1 -weighted, T_2 -weighted or diffusion weighted MRI images (Gross et al. 2017). The spatial variations of proton density, T_1 , T_2 , diffusion constant and chemical composition can be mapped with high resolution and accuracy by using MRI. Throughput is one of the limiting factors in the application of NMR/MRI for QA/QC applications. New pulse sequences are being developed for completing the data acquisition required for MRI in a short time (Stehling et al. 1991; Tyler et al. 2004).

Software/Data Analysis

FT-Based Analysis

The time-dependent response of the RF transceiver after application of an RF pulse in the presence of a magnetic field is amplified, filtered and digitized. This is known as the FID (free induction decay). The spectral response is obtained from a Discreet (Digital) Fast Fourier Transform (FFT) of the FID (Ernst and Anderson 1966), after the FID is multiplied by a window function. Although spectral data are highly informative, data acquisition with a high level of magnetic field homogeneity is required. FFT of MRI data (in k-space) is used to obtain spatial information.

Time Domain Analysis

Time domain analysis is useful for analysis of relaxation and diffusion data (Kirtil et al. 2017). If the relaxation data is expected to consist of a few components, a least squares fit to a sum of exponentials is used. If the data contains numerous components, distribution fitting methods based on kernel functions (Wilson 1992) or a Laplace transform of the time domain data provide information regarding the distribution of relaxation times. Fitting methods are available for 2D distributions of relaxation and diffusion (Mitchell et al. 2012). The relaxation times are sensitive to mobility and can be used as indicators of fruit firmness, fruit ripening, etc.

Processing of Non-linearly Sampled Data

Maximum entropy methods provide an alternative to the Fast Fourier Transform (FFT) for processing of MR data, and are especially useful for truncated or non-linearly sampled data (Mobli et al. 2006). The time domain data is directly analyzed without any windowing by using the maximum entropy principle to deal with noise in the data. If adequate S/N ratio is available, then the maximum entropy method of data analysis can result in substantial reduction in data acquisition time. A wide variety of schemes for non-linear sampling of k-space and reconstruction of MRI images from non-uniformly sampled data have been proposed (Marvasti 2012; Kojima et al. 2015) and evaluated (Lustig et al. 2007; Barriero et al. 2008).

Image Analysis

MR images can be processed rapidly to extract and analyze features of interest (Sozer 2016). Segmentation involves classification of the pixels in an image into two or more categories, such as background, healthy, diseased, etc. A variety of segmentation techniques have been used for analysis of fruit MR images, such as, region based (UPM), one dimension histogram variance thresholding (1DHVT) and two

dimensional histogram variance thresholding (2DHVT) (Barreiro et al. 2008). Regions of interest can be differentiated by using regression analysis, partial least squares, neural networks, k-means clustering, support vector machine (SVM) classifiers, etc. (Dubey and Jalal 2015). Texture analysis can be used to determine the percentage of affected and unaffected tissue (Letal et al. 2003; Szczypiński et al. 2009). The MRI images can be used to evaluate the quality of fruits and to predict the stage of fruit ripening (Letal et al. 2003), the time required for optimum ripening, the time remaining before start of degradation (rotting), etc. A substantial scope for improvement exists for development of methods for extracting useful information from low resolution MR images of fruits and/or relaxation data obtained at low magnetic field strengths (< 1 T).

Applications of Magnetic Resonance for Quality Assessment of Fruits

Magnetic resonance imaging (MRI) is useful for controlling fruits due to its non-invasive, non-destructive attributes, and its ability to provide highly resolved spatial information concerning the distribution and environment of water in soft tissues (Hancock et al. 2008). Such information has been used for non-invasive visualization of the anatomic features of fruits (Chen et al. 1989).

Magnetic resonance imaging (MRI) systems have the potential to become integral components of pre-and post-harvest investigations of physiological changes in fruits. MRI can also be used for investigation of fruit disorders during the post-harvest life of fruits (Clark et al. 1997; Clark and MacFall 2003). MRI has been used to detect the morphology, core breakdown, seeds or pits, voids, pathogen invasion, worm damage, bruises, dry regions, changes due to ripening, heating, chilling and freezing (Abbott et al. 1997; Barreiro et al. 2000; Brummell 2006).

Correlations has been observed between MR parameters and descriptors of fruit quality, such as firmness, dry matter, soluble solids content, total acidity and Brix number (Chen and Sun 1991; Dull and Birth 1989). Quantitative MR measurements can be used to grade fruits, based on sugar and/or organic acid content (Blažková et al. 2002). MRI has the potential for non-invasive assessment of the stage of ripeness, shelf-life and estimation of the optimum time for consumption. A summary of applications of MRI for fruit quality assessment is shown in Table 1. Table 2 explains the standard error and/ or coefficient of correlation values of some fruits.

Continued advancement of MRI technology, coupled with robotic positioning of fruits and computerized shimming (which involves adjustment of the homogeneity of the magnetic field)), could reduce the time and cost required for imaging and make the technique economical for specialized

markets such as superstores and food exporting organizations (Clark et al. 1997). MRI/NMR studies relevant for non-invasive assessment of fruit quality are reviewed here.

Apple (*Malus pumila*)

The variation of signal intensity in MRI images provides information on the internal structure of apple fruit, including petal bundle, endocarp, outer limit of carpel, dorsal bundle of carpel, cortex of receptacle, pith of receptacle and seeds (Wang et al. 1988). Time domain NMR and quantitative MRI can be used for investigation of the apple transformation processes in cider making technology (Rondeau-Mouro et al. 2015).

MRI can distinguish bruised and non-bruised apples image in published by Abbott (1999) because local image intensity is sensitive to diamagnetic susceptibility changes that occur in apple tissue after bruising (Abbott 1999; Wang et al. 1988). The bruised tissue regions are brighter due to greater spin-spin relaxation rates ($1/T_2$) (McCarthy et al. 1995). A fast, computerized method has been developed for detection of bruises in apples by MRI (Zion et al. 1995a).

Water core is a physiological disorder affecting apple quality in which intercellular spaces are filled with liquid. Postharvest deterioration in ‘Fuji’ apples due to watercore was monitored by using MRI (Clark et al. 1998a, b). Internal defects can be characterized by detection of cavities which are induced by elevated CO₂ and decreased O₂ levels during storage (Clark and Burmeister 1999). MRI was used to assess watercore distribution inside apple fruit and its incidence was found to be related to the effect of solar radiation inside the canopy (Melado-Herreros et al. 2013). Sugar composition, with higher fructose and total sugar contents in apples from the upper canopy were found to be significantly different compared to those in the lower canopy location. Significantly higher sorbitol and lower sucrose and fructose contents were found in watercore-affected tissue compared to the healthy tissue of affected apples and also compared to healthy apples (Melado-Herreros et al. 2013).

MRI was used to monitor and detect browning in apples during storage (Gonzalez et al. 2001). Internal browning is a physiological disorder which occurs during controlled atmospheric storage of apples. Internal browning could be detected based on differences in proton density, T₂ and diffusion coefficient. And diffusion coefficient was identified as the most appropriate parameter for detection of internal browning (Defraeye et al. 2013) (Tables 1).

MRI can determine the changes in the internal texture of intact fruits during fruit development (Faust et al. 2010). T₂ values can be used to monitor the biological state of tissues and are correlated with the ratio of bound water to free water. Marigheto et al. used novel two-dimensional NMR relaxation and diffusion techniques for study of internal sub-cellular physiological changes associated with ripening and mealiness

Table 1 Applications of MRI for characterization of fruits

Fruit name	Nature of defect	Measured attributes	References
Apple	Storage time, internal browning (IB) and degree of tissue degradation	PD, T ₂ and DC	Defraeye et al. 2013
	Disorders involving water distribution, watercore, core breakdown, chilling injury, bruising, decay, presence or feeding of insects	T ₁ and T ₂	McCarthy et al. 1995 Wang et al. 1988; Clark et al. 1998a, b
Watermelon	Internal quality via imbalances in water status, due to pressure gradients and osmotic pressure imbalance.	T ₁ PD	Sun et al. 2010 Yoshii et al. 2013
	Septa at the center of the fruits due to development of a large water potential gradient Void detection	T ₁ and T ₂	Takashi et al. 1996
Mango	Internal browning	T ₂	Elizabeth and Roy 1993
	Detection of internal defects such as bruising, chilling injury, and insect damage in Kensington Pride mango	T ₂ and DC	Mazucco et al. 1993
	Harvest stage and storage conditions. Injuries	PD and T ₂	Joyce et al. 1993; Joyce et al. 2002
Persimmon fruit	Development and post-harvest ripening stages in meso-carp parenchyma and vascular tissue	T ₁	Clark and MacFall 2003
Pears	Growth stage	T ₁	Kimura et al. 2011; Geya et al. 2013; Wang and Wang 1989; Lammertyn et al. 2003; Zhou and Li 2007
	Core breakdown	T ₁	
	Softness/firmness	Texture analysis	
Kiwifruit	Structural changes and changes in water content of pericarp due to effect of storage conditions	T ₁ and T ₂	Taglienti et al. 2009; Clark et al. 1998a, b
Blueberry and cherry peaches	Physiological and bio-chemical changes during ripening; nutrient content information Woolliness	PD, DC, Spectral imaging, ¹³ C NMR Histogram analysis of T ₂	Ishida et al. 1997; Vicente et al. 2007; Goulau and Oliveira 2008; Barreiro et al. 2000
Grapes	Organic acids and eight amino acids, internal characteristics of berries and degrees Brix distribution	T ₁ and T ₂	Andaur et al. 2004
Mandarin fruit (<i>Persea americana</i>)	Soluble solids content (SSC) sorting Flesh bruising assessment in avocados	PD T ₂ ¹ H-MRI	Barreiro et al. 2008; Mazhar et al. 2015

in apples (Marigheto et al. 2008). Proton density was observed to increase with longer storage time (Defraeye et al. 2013).

Difference in magnetic susceptibility, between gas-filled intercellular spaces and their environment inside fruit tissues, was used for quantification and for determination of the distribution of microporosity in apples (Musse et al. 2010).

Water status and distribution at subcellular level in whole apple fruit has been reported by measurement of the multi-exponential transverse (T₂) relaxation of water protons (Winisdorffer et al. 2015). MRI data regarding multi-exponential relaxation of water and apparent tissue microporosity in whole fruit were combined with histological measurements to provide a more reliable interpretation of the origin of variations in the transverse relaxation time (T₂) and better characterization of the fruit tissue.

2D T₁/T₂ global and localized relaxometry was used to perform an intensive non-destructive and non-invasive microstructure study on whole apples. The 2D T₁/T₂ cross-correlation spectroscopic studies provided quantitative information about the water compartmentation in different subcellular organelles

whereas localized relaxometry helped in predefinition of slices in order to understand the microstructure of a particular region of the fruit (Melado-Herreros et al. 2015).

A dedicated 0.2 T MRI apparatus was used for detection of infestation in apples by the peach fruit moth larvae (Haishi et al. 2011). This infestation cannot be detected at early stages by other means because the entrance holes are very small.

Watermelon (*Citrullus lanatus*)

MRI can be used to determine the internal quality of watermelon/melons (Sun et al. 2010). Healthy and defective tissues can be distinguished based on the differences in T₁ values (and proton density). Regions with defects have high free water content compared to healthy regions with low free water content. The regions of abnormal intensity in MRI images indicate the presence of defects.

Septa, in watermelons, could block the movement of water resulting in imbalances in water status and pressure gradients. Septa are partitioning tissues present in the flesh, and

Table 2 Standard error and/or coefficient of correlation values of some fruits

Fruits	Standard error/standard deviation	Correlation coefficient value	Reference
Apple	Mean value and standard deviation for mealy and non-mealy apples were 16.28 (5.29) and 22.98 (3.57), respectively. Minimum T_2 values for mealy apples were significantly lower than those for non-mealy apples ($F = 13.21$, $p < 1\%$). Histograms of T_2 maps of mealy and non-mealy apples exhibited significant differences ($F = 19.43$, $p < 1\%$)	The number of pixels below 35 ms was correlated with the deformation parameter of the Magness-Taylor firmness test (correlation coefficient $r = -0.76$).	Defraeye et al. 2013; Barreiro et al. 1999
Watermelon	Standard error of prediction (SEP) was around 0.5 using multiple regression based on T_1 and T_2 at the center of the watermelon. SEP for sugar content was below 0.858 in all regions of interest using multiple regressions based on T_1 and T_2 . Internal voids in watermelon could be detected with an accuracy of 93.3% using one dimensional MRI profiles.	Coefficient of correlation for multiple regressions at the center of the watermelon exceeded 0.9 for determination of sugar content from MRI images. Coefficient of correlation with sugar content was higher than 0.7 for determination of sugar content, in the regions of interest.	Miki et al. 1996; Saito et al. 1996
Pomegranate		Correlation coefficient (R^2) of 0.54, 0.6 and 0.63 for prediction of titratable acidity, pH and soluble acids based on T_1 , T_2 and diffusion weighted MR image data based PLS model	Zhang and McCarthy 2013
Grapes	The standard error was insignificant (<1% of the values listed) and there was no statistically significant difference (Tukey-Kramer test, $P = 0.05$) for soluble solids estimated from mean T_2 values and diffusivity maps.	The correlation of °Brix and T_1 was $R^2 = 0.75$ for Cabernet Sauvignon, $R^2 = 0.8$ for Carmenère, and $R^2 = 0.65$ for Chardonnay. This information helps in better cluster characterization.	Dean et al. 2014; Andaur et al. 2004
Mandarins	The standard deviations for seeded (S) and non-seeded (NS) fruits for Perimeter, maximum radius, compactness and aspect ratio were 28.41 (S), 14.93 (NS); 3.73 (S), 2.51(NS); 0.21 (S), 0.17(NS); and 0.19, (S), 0.06(NS) respectively, for region-based segmentation of MRI FLASH images.	Seed identification in static MRI images could be performed with 100% accuracy using radial-spiral oversampling and 98.7% accuracy with gradient echo images. The correlation coefficients between features extracted from MR image segmentation (non-invasive) and RGB image segmentation (invasive) were 0.8 for static MRI and 0.7 for dynamic MRI.	Barreiro et al. 2008; Hernandez-Sanchez et al. 2006.

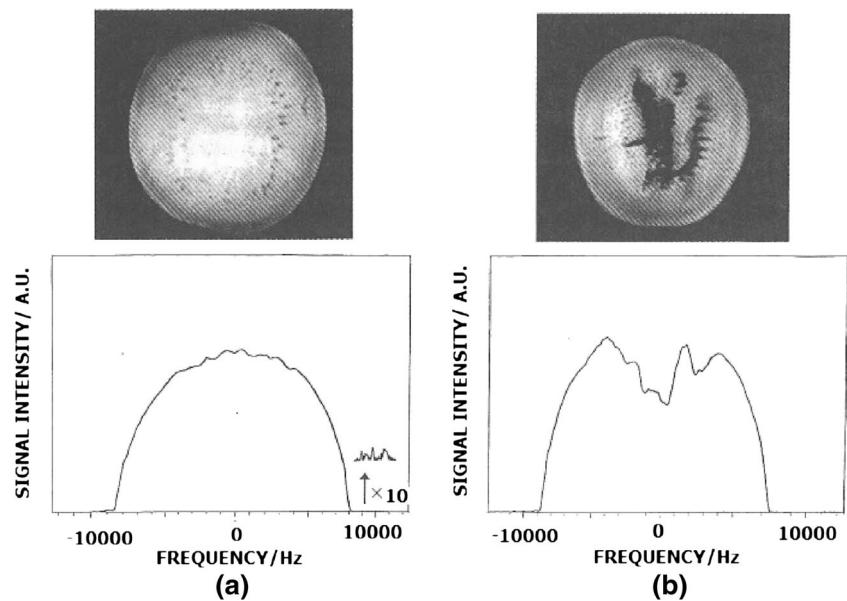
relaxation times in the septum are smaller than in other fleshy tissues. In some regions, sugar is distributed by translocation and its region of accumulation is determined by morphological factors. Differential sugar levels indicate an osmotic pressure imbalance in watermelon fruits (Yoshii et al. 2013). It could be another factor that produces the water status and pressure gradient in the fruit. MRI has revealed the disappearance of xylem and the formation of septa at the center of the fruits due to development of a large water potential gradient in hydroponically grown watermelons.

MRI can be used as a sorting machine based on analysis of sugar content and void detection in watermelons. T_1 and T_2 of intact watermelon can be used as a non-invasive, non-destructive indicator of sugar content (Takashi et al. 1996). Void detection in watermelons is possible by use of two dimensional cross sectional MRI images (Fig. 1). A 1D MRI could increase measurement rate (Saito et al. 1996). The data required for constructing one dimensional projection profiles can be acquired much more rapidly than the data required for 2D image reconstruction.

Mango (*Mangifera indica*)

MRI can be used for chemical compositional analysis and structural identification of functional components in mango. It could also help in determination of composition and formulation of packaging materials, optimization of processing parameters, and inspection of microbiological, physical and chemical quality of mangoes (Joyce et al. 2002). Areas of increased free (unbound) water or voids in the internal tissue of fruits are readily detectable by MRI and allow detection of internal defects such as bruising, chilling injury, and insect damage in mangoes (cv ‘Kensington Pride’) (Mazucco et al. 1993). Both T_2 and diffusion-weighted MRI illustrated mango tissue changes associated with internal browning (Fig. 2). Samples of mango skin could be imaged at very high spatial resolution in 11.5 or 16 Tesla microimaging systems. MRI was useful for study of the length of time between harvest and the onset of the climacteric rise in fruit respiration. It was used to study the harvest stage and the storage conditions of mango fruit which could be dependent on it.

Fig. 1 Comparison of normal and voided watermelons. **a** Normal watermelon and its MR image with its projection profile. **b** Voided watermelon and its MR image with its projection profile. There are concavities on the profiles corresponding to the voids (Saito et al. 1996)



Heat treatment, required for disinfestation, may induce injuries in mangoes. Non-destructive proton MRI was used for detecting and monitoring the progress of heat treatment-induced injury in mango fruit (Joyce et al. 1993). The injured areas have relatively low water levels (low signal intensity) corresponding to air filled cavities and “islands” of starchy mesocarp (Table 1). Heat treatment-induced lesions start to develop on the day of treatment.

^1H -MRI was used to monitor the ripening stages of ‘Kensington Pride’ mango fruit. During ripening, mesocarp tissue exhibits physico-chemical gradients. These gradients are reflected in water activity which is non-uniform throughout the mesocarp. Signal intensity in MRI (first echo, proton density and T_2) for green-mature ‘Kensington Pride’ mesocarp tissue was found highest near the endocarp and lowest near the exocarp. Water activity in the mesocarp tissue increases in an outward-moving flux as ripening progresses. It was associated with starch hydrolysis and other ripening-related processes near the endocarp (Joyce et al. 2002).

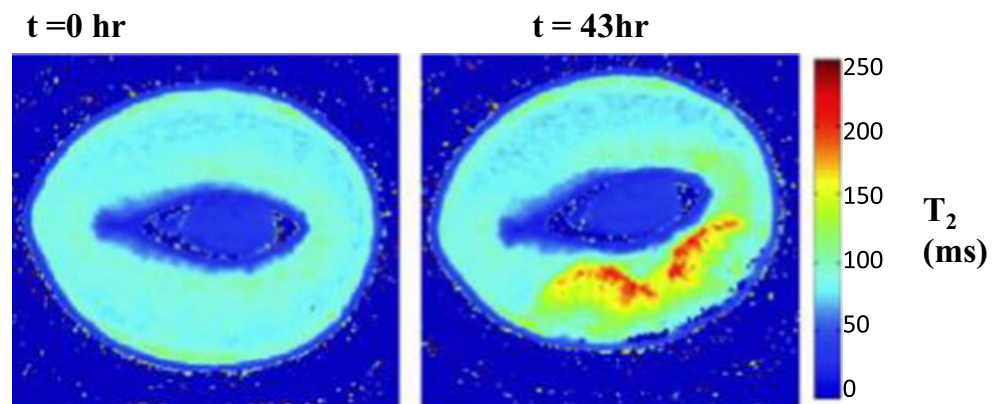
Persimmon (*Diospyros kaki*) Fruit

Qualitative and quantitative ^1H -MRI was applied for study of persimmon (*Diospyros kaki* cv ‘Fuyu’) fruit during development and post-harvest ripening stages. T_1 relaxation times in mesocarp parenchyma and vascular tissue exhibited a sigmoidal pattern of increase during the time leading to commercial harvest, but declined abruptly during ripening, 2.5 weeks after picking (Clark and MacFall 2003).

Pears (*Pyrus communis*)

MRI is a non-destructive detection method for core breakdown analysis in ‘Bartlett’ pears (Wang and Wang 1989; Geya et al. 2013). Lammertyn et al. (2000) used logistic regression to study factors that influence core breakdown in ‘Conference’ pears. Core breakdown disorder in pears, which is characterized by development of cavities and brown discoloration of tissue, is induced normally during storage

Fig. 2 Qualitative imaging (T_2 weighted) of the development of internal mango browning. Yellow and red area is mesocarp with 50–100% increase in T_2 value. It is consistent with sugar hydrolysis and decreased local sugar concentration. Image was from GE Syngo 3T MRI system with 8-channel transmit/receive knee coil (Bourme et al. 2012)



conditions, i.e., elevated CO₂ and decreased O₂ levels. MRI was able to differentiate between unaffected tissue, brown tissue and cavities. However, MRI-based estimates of the percentage of brown tissue were found to be quantitatively superior, easy and fast (Lammertyn et al. 2003; Hernández-Sánchez et al. 2007).

Firmness is an important index for the quality evaluation of fruits. Zhou and Li studied firmness of Huanghua pears, during storage, by using an artificial neural network (ANN). This ANN model, based on texture analysis of MRI images, predicted the firmness of the pears with a mean absolute error (MAE) of 0.539 N and R value of 0.969 (Zhou and Li 2007).

Nuclear magnetic resonance images of Chinese pears have been acquired by horizontal scanning mode. Image processing which included auto thresh segmentation, morphologic operation and boundary extraction by Matlab software was used to obtain an accuracy of detection for subtle bruises and other pears of 92.1 and 100%, respectively (Zhou et al. 2010).

Kimura et al. reported in situ MRI measurements of Japanese pear fruit in a research orchard using a 0.12 T permanent magnet (Kimura et al. 2011). The T₁ values of the pear fruits were measured by using the inversion recovery (IR) sequence. Geya et al. measured longitudinal NMR parameters of Japanese pear fruit by using an electrically mobile MRI system with a 0.2 T permanent magnet (Geya et al. 2013). These studies illustrate the possibility of carrying out NMR/MRI studies in the orchards before harvesting of fruits.

Low-field NMR and ¹H-MRI were used for evaluation of ‘Jinxu’ yellow peach’s storage suitability utilizing the changes in the transverse relaxation time (T₂), signal intensity (A₂), and images of ‘Jinxu’ yellow peach fruits (Zhou et al. 2016).

The Dar Gazi variety of Pear fruit is very sensitive to bruising from mechanical impact and compression. Bruised volume of pears was estimated from 3D MRI data. Applied force resulted in a linear increase in bruised volume, whereas the effect of time was non-linear (Razavi et al. 2018). The optimum time for consumption of the product, with least damage, was estimated to be 12 days after loading/unloading or external impact during harvesting and storage.

Kiwifruit (*Actinidia deliciosa*)

Quantitative MRI of kiwifruit was used to measure the relaxation parameters T₁ and T₂ during growth and ripening. They were found to remain unaltered even though there is an increase of 200% in total free sugar concentration in the flesh and 68% in the soluble solids content (Clark et al. 1998a, b). Analysis of solutions and juices showed the relaxation rates to be sensitive to increases in sugar composition but relatively insensitive to changes in organic acids and soluble pectin at concentrations normally found in fruit. There were no consistent associations with non-destructive measurements.

Fruit weight was found to decrease by 8–10% of the initial weight, due to postharvest water loss. This was accompanied by decreased relative water content (RWC) and water potential. However, no significant time-dependent change was found in the values of T₁ and T₂ measured by MRI (Burdon and Clark 2001).

Density weighted and T₂ weighted MRI was used to evaluate the effect of storage conditions, such as temperature and relative humidity, on the structural changes in kiwi tissue (Taglienti et al. 2009). Observed variations of internal morphology were correlated with T₂ of defined areas and with softening of fruits. The ability to observe time dependent changes that were unobservable in earlier studies was due to the use of a different contrast mechanism.

Blueberry (*Vaccinium corymbosum*), Cherry (*Prunus avium*) and Blackcurrant (*Ribes nigrum*)

Ishida et al. (1997) used MR density weighted images, localized spectral images and T₁ weighted images to study changes in water status and accumulation of soluble compounds in the fruit during prolonged preservation time (Table 1 and Fig. 3). The amount of water in the pericarp and seeds was found to vary inversely according to the progression of growth stages (Ishida et al. 1997).

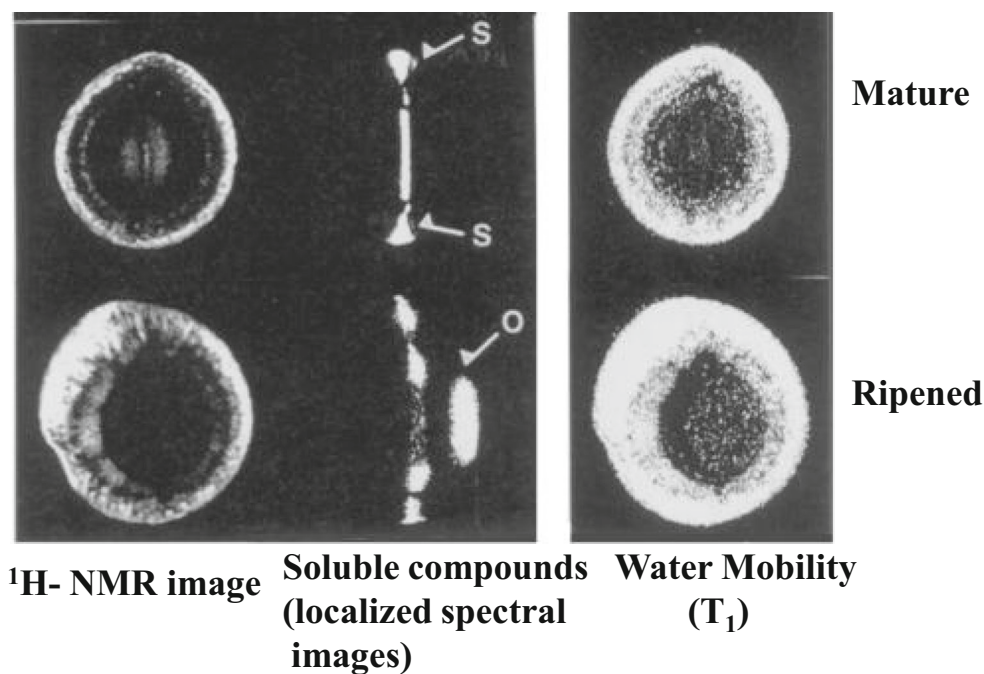
MRI can be used to detect water and sugar distribution in a single blueberry, before and after freeze/thaw (Vicente et al. 2007). Selection of either the water or the sugar signal is possible by control of the inversion recovery time (Gamble 1994). Freeze/thaw could rupture water retaining membranes within discrete locations of the fruit tissue. This causes a change in the ratio of modified water (i.e., hydrogen bonded or chemically exchanged) to unmodified (i.e. mobile and not chemically exchanged) in those regions, as well as a concomitant change in sugar concentration, due to diffusion to other tissues (Gamble 1994).

Nuclear magnetic resonance (NMR) microscopy was used for a non-invasive study the development of fruits of blackcurrant (*Ribes nigrum*) cv. Ben Alder from flower to maturity (Glidewell et al. 1999). MRI images were analyzed with additional data from low temperature scanning electron microscopy (LTSEM) and conventional resin histology. A bright core discernible in the MR image was identified as a vascular bundle whereas the darker surrounding regions were identified as small parenchyma cells with pronounced inter-cellular gas spaces.

Grapes (*Vitis vinifera*)

MRI could help in visualization of internal characteristics of berries and measurement of degrees Brix distribution within a cluster. Andaur et al. (2004) have developed calibration models to correlate soluble solids content (degrees Brix) with T₁ and T₂. They have reported the use of MRI for study of the growth and

Fig. 3 Ontogenetic changes in water and nutrient status of mature and ripened cherry fruits. This figure shows changes in proton density (left), localized spectrum (center) and relaxation weighted images (right). (Abbreviations: s= sugar and o= oils)(Ishida et al. 1997)



ripening of grape berries for three varieties: Cabernet Sauvignon, Carmenère, and Chardonnay. The correlation of degrees Brix distribution and T_1 was $R^2 = 0.75$ for Cabernet Sauvignon, $R^2 = 0.8$ for Carmenère, and $R^2 = 0.65$ for Chardonnay. Reconstruction techniques for three-dimensional representation of clusters were reported for interactive visualization of bunches (Andaur et al. 2004). The method also provides volume measurements of single berries and their distribution within the cluster with an accuracy of 3% and $R^2 = 0.98$.

Diffusion Tensor Imaging and Transverse relaxation weighted MRI were used to correlate developmental changes in grape berry tissue structure with water diffusion patterns in Semillon variety of grapes (Dean et al. 2014). Preferential directions of diffusion were observed in the inner mesocarp during the growth of the immature berries. T_2 weighted MRI revealed radial patterns connecting the vascular systems at the center of the berry with the boundary of the mesocarp.

Fruit split results in economic losses in viticulture. Diffusion MRI was used for examination and characterization of the immediate effect of fruit split on grapes. Splitting of grape berries resulted in an immediate increase in the mean apparent diffusivity in the pericarp tissue immediately surrounding the wounds (Dean et al. 2016). Standing water on the split grape berry surface results in pericarp cell death and subsequent infection.

Peaches (*Prunus persica*) and Nectarines (*Prunus persica* var. *nucipersica*)

Mealiness (woolliness in peaches) is a negative attribute of sensory texture that combines the sensation of a desegregated tissue

with the sensation of lack of juiciness. Peach mealy textures are also known as woolliness and leatheriness. Mechanical and MRI techniques were used to identify wooly peaches. MRI was also used to study the textural descriptors such as crispiness, hardness and juiciness of peaches (Barreiro et al. 2000).

MRI and X-ray computed tomography were used for evaluation of the textural characteristics of nectarines exhibiting wooly breakdown (Sonogo et al. 1995).

Mandarin (*Citrus reticulata*) Fruit

Whole-fruit MRI of Satsuma mandarin (*Citrus unshiu* Markovich cv. Miho Wase) during its maturity period was used to study anatomical changes in the peel, vascular system and juice sac morphology within pulp segments. Quantitative MR imaging was used for probing compositional changes. It was observed that there was no association between trends in the compositional changes in the MR data and total soluble solids, pH, titratable acidity, and sugar and organic acid composition of the juice (Clark and Burmeister 1999).

Magnetic resonance imaging was used to acquire images of the internal structure of mandarins for non-destructive seed identification (Barreiro et al. 2008). Several data acquisition and data analysis methods were evaluated and it was found that the best combination resulted in 100% accuracy of seed identification (Barreiro et al. 2008).

Orange (*Citrus sinensis*)

MRI was used for monitoring ripening, decay and damage in Valencia oranges which had been coated with Biorend (Galed

et al. 2004). Biorend is a preservative containing chitosan and the active film permits gradual release of preservatives for inhibition of fungal growth.

A group of 4 undamaged and 4 potentially damaged fruit were imaged at a belt speeds of 50 mm/s and 100 mm/s by using a specially designed conveyor within a 4.7 T spectrometer using FLASH MRI (Hernández-Sánchez et al. 2004). The qualities of the images were lower at the higher motion rate. Pixel based image analysis algorithms and metrics were used to assess the fruit quality.

Fruit splitting is a preharvest physiological disorder that occurs in some commercially important fruit species, such as navel oranges, Valencia oranges, and mandarins. MRI was used to study and predict the fruit splitting probability (Zur et al. 2017). The splitting could be predicted as early as 2 months before the occurrence of fruit splitting.

Strawberries (*Fragaria ananassa*)

Inversion recovery spin-echo NMR microimaging was used for studying internal physicochemical changes in flower buds and fruit of strawberry. T_1 NMR microimaging was found to be a useful tool for examining strawberry receptacles noninvasively and nondestructively while providing information on the development of receptacles. A series of T_1 -weighted inversion recovery images has greatly aided interpretation of NMR image data in terms of physical plant tissue structure and physiological processes of the tissues (Maas and Line 1995).

High field NMR microscopic imaging of parenchymal and vascular tissues in healthy strawberry fruits indicated predominantly short T_2 values. Damaged strawberry fruits from fungal pathogen *Botrytis cinerea* resulted in a large increase in T_2 in the infected tissue whereas ripening processes showed small variations in the T_2 -weighted contrast and in the relative magnitudes of T_1 between vascular and parenchymal tissue (Goodman et al. 1996).

Magnetic resonance imaging (MRI) has been used for determination of freezing injury (via exposure to 0, -8, -12, -16 and -20 °C) in strawberry crowns. The increase in signal intensity with the tissue browning of crowns dropped below -12 °C (Nestby et al. 1997).

One-dimensional MRI has been used to study the temporal and spatial changes in water mobility via T_2 profiles, water content via M_0 profiles, and structural shrinkage of strawberry slices during osmotic dehydration. MRI was useful for acquiring water mobility and moisture data for development of improved models for predicting water loss during osmotic dehydration and/or air-drying (Evans et al. 2002).

Pomegranate (*Punica granatum*)

T_2 weighted MRI slices were obtained at 1.5 T for 4 quality classes of cultivar of pomegranate Malase-e-Torsh: semi-ripe,

ripe, over-ripe and internal defects. Gray Level Cooccurrence Matrix (GLCM) and Pixel Run-Length Matrix (PRLM) parameters were used for classification. The classification accuracies have been found to be 100, 98.47, 100 and 95% for semi-ripe, ripe, over-ripe and internal defects classes, respectively. Mean classification accuracy was 95.75 and 91.28% for GLCM and PRLM features, respectively (Khoshroo et al. 2009).

Image based PLS models have been used to predict the titratable acidity, pH, and soluble solids/acidity levels (R_2 of 0.54, 0.6, and 0.63 respectively). In the PLS model, T_2 weighted Fast Spin Echo, diffusion weighted image, and Spin Echo image with short TE and moderate TR were most important for predicting the pomegranate quality attributes (Zhang and McCarthy 2013). However, the correlation between MR image statistical features and soluble solids content of pomegranate was poor.

MR Technologies Under Development and Strategies to Overcome Current Limitations

Imaging of Moving Objects

High throughput in quality control applications can be facilitated if MR signals can be acquired on moving objects (Hills and Wright 2006). The movement may involve use of a conveyor belt in continuous or 'stop and go' mode. Efficient evaluation of quality based on MRI/NMR would require that the required data are obtained in a short time, preferably in one second or less for each fruit. Modern imaging techniques such as echo-planar imaging can be utilized to acquire the complete data required for a 2D MRI image in less than one second, after an object has attained spin equilibrium in a magnetic field (Stehling et al. 1991). These experiments have been demonstrated on high resolution MRI instruments and extension to lower magnetic fields for QA/QC applications is still a challenge due to the additional requirements of fast polarization and shimming.

CPMG signals, acquired on apples transported by using a conveyor belt system through a low field MR sensor (5.55 MHz), indicated the possibility of online sorting of apples with internal browning, at speeds slower than 100 mm/s (Chayaprasert and Stroschine 2005). Prototypes of NMR/MRI systems capable of sorting fruits based on internal defects, at speeds of 10–12 m/s, have been demonstrated recently (McCarthy et al. 2016). These speeds may be sufficient for use in commercial fruit packing operations.

MRI data acquisition on continuously moving samples is feasible using new data acquisition strategies (Börnert and Aldefeld 2008) and a variety of motion artifact compensation methods. Hernandez-Sanchez et al. (2006) reported the detection of seeds in mandarins using MRI under motion conditions.

Contrast enhancement between seeds and pulp was obtained by using effective T_2 -weighted FLASH images (703 ms acquisition time). Stationary fruits were imaged and then the images were segmented to extract several features. The robustness of the motion correction procedure was evaluated by comparison of features in images acquired in static and dynamic modes (Hernandez-Sanchez et al. 2006). The acceleration and motion-correction techniques that have recently been developed for medical MRI (Hegde et al. 2015), can be utilized for MRI of fruits on conveyer belts and are expected to have a major impact on the efficiency of such applications.

Prepolarization

For many types of experiments, such as relaxation measurements and also some imaging experiments, the acquisition time is of the order of 50 ms after the sample reaches thermal (spin) equilibrium. In such cases, the sample of interest may be placed in a magnetic field to attain the required spin polarization before introduction into the active volume of the MR probe, to minimize the time spent in the probe (Verpillat et al. 2008). Physical separation of the polarization step from the data acquisition step could substantially reduce the data acquisition time per sample. The time required for movement of the object of interest into the active region of the probe and the time required to ensure absence of motion before start of acquisition may be the limiting factor in such a case.

Low Field MR and SQUID Based Detection

The bulky magnets required for MRI/NMR spectroscopy, are one of the major reasons for the limited applicability of MR in industrial applications (Kirtil et al. 2017). Therefore, attempts have been made to obtain usable MRI data with low field magnets (< 1.0 T) that have lower weight as well as lower cost. T_2 relaxation data from a low field MR sensor (0.13 T) could be used to detect internal browning and watercore in apples (Cho et al. 2008). An MRI system using a 0.2 T magnet was used for quantitative determination of water content, volume of browning tissue and internal voids in ‘Conference’ pears based on differences in spin-lattice relaxation times (Suchanek et al. 2017).

The extremely high sensitivity of the Superconducting Quantum Interference based Detector (SQUID), compared to the induction coil, permits MR studies at extremely low magnetic fields (Clarke et al. 2007). The SQUID-NMR technique has the advantage that a bulky magnet is not required, unlike the conventional methods for obtaining MRI data which require bulky magnets. MR studies of cherries at ultralow magnetic fields (<100 μ T) using high T_c SQUIDs demonstrated a high correlation between the measured spin lattice relaxation rates and sugar content (Liao and Wu 2017). The differences in the relaxation rates could be used to obtain high contrast in

SQUID based MRI. The samples can be maintained at room temperature by physical separation from the low temperature magnets. Although SQUID-based detection removes the requirement for bulky magnets, the current SQUID detectors require cooling to low temperatures and this contributes to the bulkiness of the overall system. The additional cost associated with the cooling system required for SQUID-based MR technology is a significant disadvantage that is likely to limit the potential application of this technology in food industry. The disadvantages associated with the requirements of cryogenic systems for SQUIDs can be overcome by the use of laser based Optical Pumped Atomic Magnetometers (OPAM) for detecting MRI signals (Hilschenz et al. 2017).

One-Sided MR/Unilateral MR/Ex-Situ MR

Whereas conventional NMR systems place the sample/object to be imaged within the cavity of the magnet, one-sided NMR systems are designed to study objects that are placed outside. Therefore, these systems are also called ex-situ NMR/MRI systems. Examples of such systems are the NMR-Mouse (Eidmann et al. 1996), surface-GARField (McDonald et al. 2007), Tree-Hugger (Jones et al. 2012) and NMR/MRI systems designed for petroleum logging e.g. CMR (Allen et al. 1997), MRIL tool (Coates et al. 1999). The advantage of this mode of imaging is that objects that are much larger than the magnet can be studied, because they can be placed outside the magnet (Utsuzawa and Fukushima 2017).

Lab-On-Chip NMR

Decrease in the size and weight contribute substantially to the ease of use as well as reduction in total cost of the instruments. Substantial progress in the miniaturization of the NMR/MRI subcomponents has been achieved by the demonstration of an NMR transceiver on a chip (Sun et al. 2009). A Palm-NMR system that weighs only 0.1 kg has been demonstrated that is based on a 0.56 T magnet, a high quality solenoidal coil and a CMOS-based NMR transceiver. Furthermore, a 1-chip NMR system that incorporates an NMR coil along with the NMR transceiver on to the same chip has also been demonstrated (Sun et al. 2011). However, these systems require small sized samples.

Multiple Transmit/Receive Coils

MR imagers equipped with multiple transmit/receive coils permit multiplexed data acquisition and are currently being used for medical applications to reduce total acquisition time (Vernickel et al. 2007). For applications involving QA/QC of fruits, such technology would permit simultaneous imaging of multiple fruits leading to higher throughput. This would be particularly useful for an experimental setup involving a

stop-and-go type of conveyer belt. Use of multiple T/R coils would permit data acquisition on multiple samples in each stop-and-go cycle. The ability to obtain data on multiple samples at the same time would permit use of longer stop time for each per sample, which can be utilized for optimal shimming and polarization. This will not decrease the overall throughput, because the overall throughput in this case would be the cycle time divided by the number of samples imaged in one stop and go cycle. The time required for shimming and for polarization of the sample are often the limiting factors in acquisition of MR data on moving samples. 3D MRI can be accelerated by scanning contiguous volumes rather than sequential slices (Hamilton et al. 2017).

Conclusion

The applications reviewed in this article demonstrate the applicability of MRI for identification of defects, for quality assessment and for determination of the stage of ripening in apples, watermelons, oranges, mangoes, cherries, peaches, pears, grapes, strawberries and pomegranates. Although a variety of other non-invasive techniques are available for evaluation of fruit quality and stage of ripening, most of them are applicable only for evaluation of a specific property for a specific type of fruit. The wide variety of MR measurable properties, such as proton density, chemical shifts, T_1 , T_2 and diffusion constant, and the ability to measure their 2D and 3D spatial distribution, enable us to design a wide variety of assays that can be applied to assess different types of defects, stress and physiological states of fruits, which are indicators of quality and provide information regarding optimum time for consumption.

The throughput, and the size, weight, cost and stability of magnets is currently the major limitation for wider application of MR-based technology for non-invasive QA/QC of fruits. A throughput exceeding 1 fruit per second, deemed to be necessary for QA/QC applications of fruits, can be achieved for proton density or relaxation weighted 2D MRI (Hernandez-Sanchez et al. 2006). It may also be feasible to acquire diffusion weighted or chemical shift selective 2D MRI with the necessary throughput. 3D MRI and MRSI can provide additional diagnostic information, however, acquisition times are considerably higher than those for 2D MRI. Although NMR microimaging provides detailed information regarding internal structures, it requires higher magnetic field homogeneity and is more susceptible to motion artifacts than conventional MRI. Heteronuclear MRI requires considerably more time or higher magnetic fields than ^1H MRI, because of the low abundance (1.1%) of ^{13}C isotope in native fruits.

The most promising technologies, in the near term, that have the potential to extend the applications of magnetic resonance for evaluation of the quality of fruits and for prediction

of the state of ripening are low field MRI, mobile MRI, prepolarization and MRI of objects moving on a conveyer belt coupled with techniques for compensation of motion artifacts. Continuous improvement in the sensitivity of RF electronics, pulse sequences and data analysis methods will continue to extend the range of applications.

Compliance with Ethical Standards

Conflict of Interest R. K. Srivastava declares that he has no conflict of interest. S. Talluri declares that he has no conflict of interest. Sk. Khasim Beebi declares that he has no conflict of interest. B. Rajesh Kumar declares that he has no conflict of interest.

Ethical Approval This article does not contain any studies with human participants or animals performed by any of the authors.

Informed Consent Informed consent is not obtained from all individual participants included in the study.

References

- Abbott JA (1999) Quality measurement of fruits and vegetables. *Postharvest Biol. Technol.* 15(3):207–225. [https://doi.org/10.1016/S0925-5214\(98\)00086-6](https://doi.org/10.1016/S0925-5214(98)00086-6)
- Abbott JA, Lu R, Upchurch BL, Stroshine RL (1997) Technologies for non-destructive quality evaluation of fruits and vegetables. In: Janicke J (ed) *Horticultural reviews* 20. John Wiley & Sons, Inc., Oxford. <https://doi.org/10.1002/9780470650646.ch1>
- Allen DF, Crary S, Freedman R, Andreani M, Klopff W, Badry R, Flaum C, Kenyon WE, Kleinberg RL, Gossenberger R, Horkowitz D, Logan P, Singer J, White J (1997) How to use borehole nuclear magnetic resonance. *Schlumberger Oilfield Rev* 9(2):34–57 https://www.slb.com/~media/Files/resources/oilfield_review/ors97/sum97/borehole.pdf
- Andaur JE, Guesalaga AR, Agosin EE, Guarini MW, Irrarrazaval P (2004) Magnetic resonance imaging for non-destructive analysis of wine grapes. *J Agric Food Chem* 52(2):165–170. <https://doi.org/10.1021/jf034886c>
- Arendse E, Fawole OA, Magwaza LS, Opara UL (2018) Non-destructive prediction of internal and external quality attributes of fruit with thick rind: a review. *J Food Eng* 217:11–23. <https://doi.org/10.1016/j.jfoodeng.2017.08.009>
- Barreiro P, Ruiz-Cabello J, Fernández-Valle ME, Ortiz C, Ruiz-Altisent M (1999) Mealiness assessment in apples using MRI techniques. *Magn Reson Imaging* 17(2):275–281. [https://doi.org/10.1016/S0730-725X\(98\)00160-X](https://doi.org/10.1016/S0730-725X(98)00160-X)
- Barreiro P, Ortiz C, Ruiz-Cabello M, Fernández-Valle ME, Recasens I, Asensio M (2000) Mealiness assessment in apples and peaches using MRI techniques. *Magn Reson Imaging* 18(9):1175–1181. [https://doi.org/10.1016/S0730-725X\(00\)00179-X](https://doi.org/10.1016/S0730-725X(00)00179-X)
- Barreiro P, Zheng C, Sun DW, Hernández-Sánchez N, Pérez-Sánchez JM, Ruiz-Cabello J (2008) Non-destructive seed detection in mandarins: comparison of automatic threshold methods FLASH and COMSPIRA MRIs. *Postharvest Biol Technol* 47(2):189–198. <https://doi.org/10.1016/j.postharvbio.2007.07.008>
- Blažková J, Hlušíčková I, Blažek J (2002) Fruit weight, firmness and soluble solids content during ripening of Karešova Cv. Sweet cherry. *Hort Sci (Prague)* 29(3):92–98 <http://agris.fao.org/agris-search/search.do?recordID=CZ2003000088>

- Bloch F, Hansen WW, Packard M (1946) Nuclear induction. *Phys Rev* 69(3–4):127. <https://doi.org/10.1103/PhysRev.69.127>
- Bloembergen N, Purcell EM, Pound RV (1948) Relaxation effects in nuclear magnetic resonance absorption. *Phys Rev* 73:679. <https://doi.org/10.1103/PhysRev.73.679>
- Blumich B (2016) Introduction to compact NMR: a review of methods. *Trends Anal Chem* 83:2–11. <https://doi.org/10.1016/j.trac.2015.12.012>
- Bömer P, Aldefeld B (2008) Principle of whole-body continuously moving table MRI. *J Magn Reson Imaging* 28(1):1–12. <https://doi.org/10.1002/jmri.21339>
- Bottomley PA (1982) NMR imaging techniques and applications: a review. *Rev Sci Instrum* 53:1319. <https://doi.org/10.1063/1.1137180>
- Bottomley PA, Griffiths JR (eds) (2016) Handbook of magnetic resonance spectroscopy in vivo: MRS theory and applications., eMagRes. Wiley, Hoboken <http://as.wiley.com/WileyCDA/WileyTitle/productCd-1118997662.html>
- Bourne MR, Banos C, Davies JB, Banati R, Henriod R (2012) Non-destructive assessment of gamma irradiation on internal mango quality. Image courtesy of the Australian Nuclear Science and Technology Organisation (ANSTO). ACS013091. <http://www.ansto.gov.au/AboutANSTO/MediaCentre/News/ACS013091>
- Brant WE, de Lange EE (eds) (2012) Essentials of body MRI. Oxford University Press, Oxford <https://global.oup.com/academic/product/essentials-of-body-mri-9780199738496?cc=id&lang=en&#>
- Brown RW, YCN C, Haacke EM, Thompson MR, Venkatesan R (eds) (2014) Magnetic Resonance Imaging: Physical principles and sequence design, 2nd edn. Wiley, Hoboken <http://as.wiley.com/WileyCDA/WileyTitle/productCd-0471720852.html>
- Brummell DA (2006) Cell wall disassembly in ripening fruit. *Funct Plant Biol* 33(2):103–119. <https://doi.org/10.1071/FP05234>
- Burdon J, Clark CJ (2001) Effect of postharvest water loss on 'Hayward' kiwifruit water status. *Postharvest Biol Technol* 22(3):215–225. [https://doi.org/10.1016/S0925-5214\(01\)00095-3](https://doi.org/10.1016/S0925-5214(01)00095-3)
- Butz P, Hofmann C, Tauscher B (2005) Recent developments in non-invasive techniques for fresh fruit and vegetable internal quality analysis. *J Food Sci* 70(9):131–141. <https://doi.org/10.1111/j.1365-2621.2005.tb08328.x>
- Bydder GM, Young IR (1985) MR imaging: clinical use of the inversion recovery sequence. *J Comput Assist Tomogr* 9(4):659–675 http://mriquestions.com/uploads/3/4/5/7/34572113/mrimaging_clinical_use_of_the_inversion_recovery.2.pdf
- Callaghan PT, Clark CJ, Forde LC (1994) Use of static and dynamic NMR microscopy to investigate the origins of contrast in images of biological tissues. *Biophys Chem* 50:225–235. [https://doi.org/10.1016/0301-4622\(94\)85034-8](https://doi.org/10.1016/0301-4622(94)85034-8)
- Carr HY, Purcell EM (1954) Effects of diffusion on free precession in nuclear magnetic resonance experiments. *Phys Rev* 94:630–638. <https://doi.org/10.1103/PhysRev.94.630>
- Chayaprasert W, Strohshine R (2005) Rapid sensing of internal browning in whole apples using a low-cost, low-field proton magnetic resonance sensor. *Postharvest Biol Technol* 36(3):291–301. <https://doi.org/10.1016/j.postharvbio.2005.02.006>
- Chen P, Sun Z (1991) A review of non-destructive methods for quality evaluation and sorting of agricultural products. *J Agric Eng Res* 49: 85–98. [https://doi.org/10.1016/0021-8634\(91\)80030-1](https://doi.org/10.1016/0021-8634(91)80030-1)
- Chen P, McCarthy MJ, Kauten R (1989) NMR for internal quality evaluation of fruits and vegetables. *Trans Am Soc Agric Eng (ASAE)* 32(5):1747–1753. <https://doi.org/10.13031/2013.31217>
- Cheng YC, Lin TT, Chou CY, Chen JH (2008) Physico-chemical analysis of internal bruise of selected fruits using chemical shift imaging. Conference, Providence, Rhode Island, 084545. <https://doi.org/10.13031/2013.25010>
- Cho BK, Chayaprasert W, Strohshine RL (2008) Effect of internal browning and watercore on low field (5.4 MHz) proton magnetic resonance measurement of T₂ value of whole apples. *Postharvest Biol Technol* 47:81–89. <https://doi.org/10.1016/j.postharvbio.2007.05.018>
- Chudek JA, Hunter G (2002) Stray field (STRAFI) and single point (SPI) magnetic resonance imaging. *Annu Rep NMR Spectrosc* 45:151–187. [https://doi.org/10.1016/S0066-4103\(02\)45011-9](https://doi.org/10.1016/S0066-4103(02)45011-9)
- Clark CJ, Burmeister DM (1999) Magnetic resonance imaging of Browning development in 'Braeburn' apple during controlled atmosphere storage under high CO₂. *HortSci* 34(5):915–919 <http://hortsci.ashspublishations.org/content/34/5/915.abstract>
- Clark CJ, MacFall JS (2003) Quantitative magnetic resonance imaging of 'Fuyu' persimmon fruit during development and ripening. *Magn Reson Imaging* 21(6):679–685. [https://doi.org/10.1016/S0730-725X\(03\)00082-1](https://doi.org/10.1016/S0730-725X(03)00082-1)
- Clark CJ, Hockings PD, Joyce DC, Mazucco RA (1997) Application of magnetic resonance imaging to pre- and post-harvest studies of fruits and vegetables. *Postharvest Biol Technol* 11(1):1–21. [https://doi.org/10.1016/S0925-5214\(97\)01413-0](https://doi.org/10.1016/S0925-5214(97)01413-0)
- Clark CJ, Drummond LN, MacFall JS (1998a) Quantitative NMR imaging of kiwifruit (*Actinidia deliciosa*) during growth and ripening. *J Sci Food Agric* 78(3):349–358. [https://doi.org/10.1002/\(SICI\)1097-0010\(199811\)78:3<349::AID-JSFA125>3.0.CO;2-X](https://doi.org/10.1002/(SICI)1097-0010(199811)78:3<349::AID-JSFA125>3.0.CO;2-X)
- Clark CJ, MacFall JS, Bielecki RL (1998b) Loss of watercore from 'Fuji' apple observed by magnetic resonance imaging. *Sci Hortic* 73(4): 213–227. [https://doi.org/10.1016/S0304-4238\(98\)00076-4](https://doi.org/10.1016/S0304-4238(98)00076-4)
- Clarke J, Hatridge M, Möble M (2007) SQUID-detected magnetic resonance imaging in microtesla fields. *Ann Rev Biomed Eng* 9:389–413. <https://doi.org/10.1146/annurev.bioeng.9.060906.152010>
- Coates GR, Xiao L, Prammer MG (eds) (1999) NMR Logging, Principles and Applications, 1st edn. Halliburton Energy Services, (1–234), Gulf Publishing Company, Houston http://www.halliburton.com/public/lp/contents/Books_and_Catalogs/web/NMR-Logging-Principles-and-Applications.Halli-burton-Energy-Services/9780967902609
- Colnago LA, Andrade FD, Souza AA, Azeredo RBV, Lima AA, Cerioni LM, Osan TM, Pusiol DJ (2014) Why is inline NMR rarely used as industrial sensor? Challenges and opportunities. *Chem Eng Technol* 37(2):191–203. <https://doi.org/10.1002/ceat.201300380>
- Constantinesco A, Choquet P, Cauffet G, Fournier JM, Ravier S, Drillon JM, Aubert G (1998) Low-field dedicated and desktop magnetic resonance imaging systems for agricultural and food applications. *Magn Reson Chem* 35:S69–S75. [https://doi.org/10.1002/\(SICI\)1097-458X\(199712\)35:13<S69::AID-OMR198>3.0.CO;2-5](https://doi.org/10.1002/(SICI)1097-458X(199712)35:13<S69::AID-OMR198>3.0.CO;2-5)
- Danieli E, Perlo J, Blumich B, Casanova F (2010) Small magnets for portable NMR spectrometers. *Angew Chem Int Ed* 49(24):4133–4135. <https://doi.org/10.1002/anie.201000221>
- Dean RJ, Stait-Gardner T, Clarke SJ, Rogiers SY, Bobek G, Price WS (2014) Use of diffusion magnetic resonance imaging to correlate the developmental changes in grape berry tissue structure with water diffusion patterns. *Plant Methods* 10(1):35. <https://doi.org/10.1186/1746-4811-10-35>
- Dean RJ, Bobek G, Stait-Gardner T, Clarke SJ, Rogiers SY, Price WS (2016) Time-course study of grape berry split using diffusion magnetic resonance imaging. *Aust J Grape Wine Res* 22:240–244. <https://doi.org/10.1111/ajgw.12184>
- Defraeye T, Lehmann V, Carolin DG, Herremans HE, Verboven P, Verlinden BE, Nicolai BM (2013) Application of MRI for tissue characterisation of 'Braeburn' apple. *Postharvest Biol Technol* 75: 96–105. <https://doi.org/10.1016/j.postharvbio.2012.08.009>
- Dickinson WC (1950) Dependence of the F19 nuclear resonance position on chemical compound. *Phys Rev* 77:736–737. <https://doi.org/10.1103/PhysRev.77.736.2>
- Dubey SR, Jalal AS (2015) Application of image processing in fruit and vegetable analysis: a review. *J Intell Syst* 24(4):405–424. <https://doi.org/10.1515/jisys-2014-0079>
- Dull GG, Birth GS (1989) Nondestructive evaluation of fruit quality: use of near-infrared spectrophotometry to measure soluble solids in

- intact honeydew melons. *HortSci* 24:754–758 <http://agris.fao.org/agris-search/search.do?recordID=US9016249>
- Eidmann G, Savelsberg R, Blümmler P, Blümlich B (1996) The NMR mouse, a mobile universal surface explorer. *J Magn Reson Ser A* 122(1):104–109. <https://doi.org/10.1006/jmra.1996.0185>
- Elizabeth JM, Roy EM (1993) Respiration rate, internal atmosphere, and ethanol and acetaldehyde accumulation in heat-treated mango fruit. *Postharvest Biol Technol* 3(1):77–86. [https://doi.org/10.1016/0925-5214\(93\)90029-3](https://doi.org/10.1016/0925-5214(93)90029-3)
- Ernst RR, Anderson WA (1966) Application of Fourier transforms spectroscopy to magnetic resonance. *Rev Sci Instrum* 37:93–102. <https://doi.org/10.1063/1.1719961>
- Evans SD, Brambill A, Lane DM, Torreggiani D, Hall LD (2002) Magnetic resonance imaging of strawberry (*Fragaria vesca*) slices during osmotic dehydration and air drying. *LWT - Food Sci Technol* 35(2):177–184. <https://doi.org/10.1006/food.2001.0830>
- Farhat IA, Belton PS, Webb GA (eds) (2007) *Magnetic resonance in food science: from molecules to man*. RSC Publishing, Cambridge <http://pubs.rsc.org/en/Content/eBook/978-0-85404-340-8>
- Faust M, Wang PC, Maas J (2010) The use of magnetic resonance imaging in plant science. *Hortic Rev* 20:225–266. <https://doi.org/10.1002/9780470650646.ch3>
- Fuchs J, Neuberger T, Rolletschek H, Schiebold S, Nguyen TH, Borisjuk N, Borner A, Melkus G, Jakob P, Borisjuk L (2013) A noninvasive platform for imaging and quantifying oil storage in submillimeter tobacco seed. *Plant Physiol* 161(2):573–593. <https://doi.org/10.1104/pp.12.210062>
- Fukushima E, Roeder SPW (1993) *Experimental pulse NMR: a nuts and bolts approach*. Westview Press, Boulder <https://www.amazon.in/Experimental-Pulse-NMR-Eiichi-Fukushima/dp/0201627264>
- Galed G, Fernandez-Valle ME, Martinez A, Heras A (2004) Application of MRI to monitor the process of ripening and decay in citrus treated with chitosan solutions. *Magn Reson Imaging* 22(1):127–137. <https://doi.org/10.1016/j.mri.2003.05.006>
- Gamble GR (1994) Non-invasive determination of freezing effects in blueberry fruit tissue by magnetic resonance imaging. *J Food Sci* 59(3):571–573. <https://doi.org/10.1111/j.1365-2621.1994.tb05564.x>
- Geya Y, Kimura T, Fujisaki H, Terada Y, Kose K, Haishi T, Gemma H, Sekozawa Y (2013) Longitudinal NMR parameter measurements of Japanese pear fruit during the growing process using a mobile magnetic resonance imaging system. *J Magn Reson* 226:45–51. <https://doi.org/10.1016/j.jmr.2012.10.012>
- Glidewell SM, Williamson B, Duncan GH, Chudek JA, Hunter G (1999) The development of blackcurrant fruit from flower to maturity: a comparative study by 3D nuclear magnetic resonance (NMR) micro-imaging and conventional histology. *New Phytol* 141(1):85–98. <https://doi.org/10.1046/j.1469-8137.1999.00319.x>
- Gonzalez JJ, Valle RC, Bobroff S, Biasi WV, Mitcham EJ, MacCarthy MJ (2001) Detection and monitoring of internal browning in 'Fuji' apples using MRI. *Postharvest Biol Technol* 22(2):179–188. [https://doi.org/10.1016/S0925-5214\(00\)00183-6](https://doi.org/10.1016/S0925-5214(00)00183-6)
- Goodman BA, Williamson B, Simpson EJ, Chudek JA, Hunter G, Prio DAM (1996) High field nmr microscopic imaging of cultivated strawberry fruit. *Magn Reson Imaging* 14(2):187–196. [https://doi.org/10.1016/0730-725X\(95\)02051-T](https://doi.org/10.1016/0730-725X(95)02051-T)
- Goulao LF, Oliveira CM (2008) Cell wall modifications during fruit ripening: when a fruit is not the fruit. *Trends in Food Sci. Technol.* 19:4–25. <https://doi.org/10.1016/j.tifs.2007.07.002>
- Gromova M, Guillermo A, Bayle PA, Bardet M (2016) In situ studies of plant seeds using ^{13}C or ^1H MAS NMR and ^1H PFG NMR approaches. In: Webb G (ed) *Modern Magnetic Resonance*. Springer, Berlin, pp 1–16. https://doi.org/10.1007/978-3-319-28275-6_18-1
- Gross D, Zick K, Guthausen G (2017) Recent MRI and diffusion studies of food structures. *Annu Rep NMR Spectrosc* 90:145–197. <https://doi.org/10.1016/bs.armr.2016.09.001>
- Gunasekaran S (ed) (2000) *Non-destructive food evaluation: Techniques to analyze properties and quality*. Food science series, 1st edn. CRC Press, Boca Raton <https://www.crcpress.com/Nondestructive-Food-Evaluation-Techniques-to-Analyze-Properties-and-Quality/Gunasekaran/p/book/9780824704537>
- Haishi T, Koizumi H, Arai T, Koizumi M, Kano H (2011) Rapid detection of infestation of apple fruits by the peach fruit moth, *Carposina sasakii* Matsumura, larvae using a 0.2-T dedicated magnetic resonance imaging apparatus. *Appl Magn Reson* 41(1):1–18. <https://doi.org/10.1007/s00723-011-0222-8>
- Hamilton J, Franson D, Seiberlich N (2017) Recent advances in parallel imaging for MRI. *Prog Nucl Magn Reson Spectrosc* 101:71–95. <https://doi.org/10.1016/j.pnmrs.2017.04.002>
- Hancock J, Callow P, Serce S, Hanson E, Beaudry R (2008) Effect of cultivar, controlled atmosphere storage, and fruit ripeness on the long-term storage of highbush blueberries. *HortTechnology* 18(2):199–205 <http://horttech.Ashspublishations.org/content/18/2/199.full>
- Hegde SS, Zhang Y, Bottomley PA (2015) Acceleration and motion-correction techniques for high-resolution intravascular MRI. *Magn Reson Med* 74(2):452–461. <https://doi.org/10.1002/mrm.25436>
- Heidenreich M, Spyros A, Kockenbeger W, Chandrakumar N, Bowtell R, Kimmich R (2008) CYCLCROP mapping of ^{13}C labelled compounds: perspectives in polymer science and plant physiology. *Spatially Resolved Magnetic Resonance: Methods, Materials, Medicine, Biology, Rheology, Geology, Ecology, Hardware*. Ed. Blumler P, Blumlich B, Botto R, Fukushima E. pp.21–52. <https://doi.org/10.1002/9783527611843.ch02>
- Hernández-Sánchez N, Barreiro P, Ruiz-Altisent M, Ruiz-Cabello J, Encarnación Fernández-Valle M (2004) Detection of freeze injury in oranges by magnetic resonance imaging of moving samples. *Appl Magn Reson* 26:431–445. <https://doi.org/10.1007/BF03166814>
- Hernandez-Sanchez N, Barreiro P, Ruiz-Cabello J (2006) On-line identification of seeds in mandarins with magnetic resonance imaging. *Biosyst Eng* 95(4):529–536. <https://doi.org/10.1016/j.biosystemseng.2006.08.011>
- Hernández-Sánchez N, Hills B, Barreiro BP, Marigheto N (2007) An NMR study on internal browning in pears. *Postharvest Biol Technol* 44(3):260–270. <https://doi.org/10.1016/j.postharvbio.2007.01.002>
- Hills BP, Wright KM (2006) Motional relativity and industrial NMR sensors. *J Magn Reson* 178(2):193–205. <https://doi.org/10.1016/j.jmr.2005.09.010>
- Hilschenz I, Ito Y, Natsukawa H, Oida T, Yamamoto T, Kobayashi T (2017) Remote detected low-field MRI using an optically pumped atomic magnetometer combined with a liquid cooled prepolarization coil. *J Magn Reson* 274:89–94. <https://doi.org/10.1016/j.jmr.2016.11.006>
- Ishida N, Ogawa H, Koizumi M, Kano H (1997) Ontogenic changes of the water status and accumulated soluble compounds in growing cherry fruits studied by NMR imaging. *Magn Reson Chem* 35(13):S22–S28. [https://doi.org/10.1002/\(SICI\)1097-458X\(199712\)35:13<S22::AID-OMR206>3.0.CO;2-5](https://doi.org/10.1002/(SICI)1097-458X(199712)35:13<S22::AID-OMR206>3.0.CO;2-5)
- Jones M, Aptaker PS, Cox J, Gardiner BA, McDonald PJ (2012) A transportable magnetic resonance imaging system for in situ measurements of living trees: the tree hugger. *J Magn Reson* 218:133–140. <https://doi.org/10.1016/j.jmr.2012.02.019>
- Joyce DC, Hockings PD, Mazucco RA, Shorter AJ, Brereton IM (1993) Heat treatment injury of mango fruit revealed by nondestructive magnetic resonance imaging. *Postharvest Biol Technol* 3(4):305–311. [https://doi.org/10.1016/0925-5214\(93\)90011-Q](https://doi.org/10.1016/0925-5214(93)90011-Q)
- Joyce DC, Hockings PD, Mazucco RA, Shorter AJ (2002) ^1H -Nuclear magnetic resonance imaging of the ripening of 'Kensington Pride' mango fruit. *Funct Plant Biol* 29(7):873–879. <https://doi.org/10.1071/PP01150>

- Keeler J (2013) Understanding NMR spectroscopy, 2nd edn. Wiley, Hoboken <http://as.wiley.com/WileyCDA/WileyTitle/productCd-0470746084.html>
- Khoshroo A, Keyhani A, Zoroofi RA, Rafiee S, Zamani Z, Alsharif MR (2009) Classification of pomegranate fruit using texture analysis of MR images. *Agric Eng Int CIGR EJ* XI:1182 <http://www.cigrjournal.org/index.php/Ejournal/article/view/1182/1166>
- Kimura T, Geya Y, Terada Y, Kose K, Haishi T, Gemma H, Sekozawa Y (2011) Development of a mobile magnetic resonance imaging system for outdoor tree measurements. *Rev Sci Instrum* 82(5):053704. <https://doi.org/10.1063/1.3589854>
- Kirtıl E, Cikricki S, McCarthy MJ, Oztop MH (2017) Recent advances in time domain NMR and MRI sensors and their food applications. *Curr Opin Food Sci* 17:9–15. <https://doi.org/10.1016/j.cofs.2017.07.005>
- Koizumi M, Naito S, Ishida N, Haishi T, Kano H (2008) A dedicated MRI for food science and agriculture. *Food Sci Technol Res* 14(1):74–82. <https://doi.org/10.3136/fstr.14.74>
- Kojima S, Shinohara H, Hashimoto T, Hirata M, Ueno E (2015) Iterative image reconstruction that includes a total variation regularization for radial MRI. *Radiol Phys Technol* 8(2):295–304. <https://doi.org/10.1007/s12194-015-0320-7>
- Kumar A, Welti D, Ernst RR (1975) NMR Fourier Zeugmatography. *J Magn Reson* 18(1):69–83. [https://doi.org/10.1016/0022-2364\(75\)90224-3](https://doi.org/10.1016/0022-2364(75)90224-3)
- Lammertyn J, Aerts M, Verlindern BE, Schotmans W, Nicolai BM (2000) Logistic regression of factors influencing core breakdown in ‘Conference’ pears. *Postharvest Biol Technol* 20(1):25–37. [https://doi.org/10.1016/S0925-5214\(00\)00114-9](https://doi.org/10.1016/S0925-5214(00)00114-9)
- Lammertyn J, Dresselaers T, Van Hecke P, Jancsó P, Wevers M, Nicolai BM (2003) MRI and X-ray CT study of spatial distribution of core breakdown in ‘conference’ pears. *Magn Reson Imaging* 21(7):805–815. [https://doi.org/10.1016/S0730-725X\(03\)00105-X](https://doi.org/10.1016/S0730-725X(03)00105-X)
- Lauterbur PC (1973) Image formation by induced local interactions: examples employing nuclear magnetic resonance. *Nature* 242:190–191. <https://doi.org/10.1038/242190a0>
- Letal J, Jirak D, Suderlova L, Hajek M (2003) MRI texture analysis of MR images during ripening and storage. *LWT Food Sci Technol* 36(7):719–727. [https://doi.org/10.1016/S0023-6438\(03\)00099-9](https://doi.org/10.1016/S0023-6438(03)00099-9)
- Liao SH, Wu PC (2017) A study of spin–lattice relaxation rates of glucose, fructose, sucrose and cherries using high-Tc SQUID-based NMR in ultralow magnetic fields. *Supercond Sci Technol* 30(08):084006. <https://doi.org/10.1088/1361-6668/aa73ab>
- Lustig M, Donoho D, Pauly JM (2007) Sparse MRI: the application of compressed sensing for rapid MR imaging. *Magn Reson Med* 58(6):1182–1195. <https://doi.org/10.1002/mrm.21391>
- Maas JL, Line MJ (1995) Nuclear magnetic resonance microimaging of strawberry flower buds and fruit. *Hortscience* 30(5):1090–1096 <https://geoscience.net/research/002/662/002662699.php>
- Marcone MF, Wang S, Albabish W, Nie S, Somnarain D, Hill A (2013) Diverse food based applications of nuclear magnetic resonance (NMR) technology. *Food Res Int* 51(2):729–747. <https://doi.org/10.1016/j.foodres.2012.12.046>
- Marigheto N, Venturi L, Hiells B (2008) Two-dimensional NMR relaxation studies of apple quality. *Postharvest Biol Technol* 48(3):331–340. <https://doi.org/10.1016/j.postharvbio.2007.11.002>
- Marvasti F (2012) Nonuniform sampling: theory and practice. Springer US. Kluwer Academic/Plenum Publishers, New York, <http://www.springer.com/in/book/9780306464454>
- Mazhar M, Joyce D, Cowin G, Brereton I, Hofman P, Collins R, Gupta M (2015) Non-destructive ¹H-MRI assessment of flesh bruising in avocado (*Persea americana* m.) cv. hass. *Postharvest Biol Technol* 100:33–40. <https://doi.org/10.1016/j.postharvbio.2014.09.006>
- Mazucco RA, Joyce DC, Hockings PD (1993) Magnetic resonance imaging applied to harvested mango fruit. *Austral Postharvest Conf. C.S.I.R.O. Div. Horticulture* 1119:355–358
- McCarthy MJ, Zion B, Chen P, Ablett S, Darke AH, Lilliford PJ (1995) Diamagnetic susceptibility changes in apple tissue after bruising. *J Sci Food Agric* 67(1):13–20. <https://doi.org/10.1002/jsfa.2740670103/abstract>
- McCarthy MJ, Zhang L, McCarthy KL, Coulthard T (2016) Status and future of magnetic resonance imaging sensors for in-line assessment and sorting of fruit. *Acta Hort* (1119):121–126. <https://doi.org/10.17660/ActaHortic.2016.1119.16>
- McDonald PJ, Ciampi E, Keddie J, Heidenreich M, Kimmich R (1999) Magnetic-resonance determination of the spatial dependence of the droplet size distribution in teh cream layer of oil-in-water emulsions: evidence for the effects of depletion flocculation. *Phys Rev E* 59:874. <https://doi.org/10.1103/PhysRevE.59.874>
- McDonald PJ, Aptaker PS, Mitchell J, Mulheron M (2007) A unilateral NMR magnet for sub-structure analysis in the built environment: the surface GARField. *J Magn Reson* 185(1):1–11. <https://doi.org/10.1016/j.jmr.2006.11.001>
- Melado-Herreros A, Muñoz-García MA, Blanco A, Val J, Fernández-Valle ME, Barreiro P (2013) Assessment of watercore development in apples with MRI: effect of fruit location in the canopy. *Postharvest Biol Technol* 86:125–133. <https://doi.org/10.1016/j.postharvbio.2013.06.030>
- Melado-Herreros A, Fernández-Valle ME, Barreiro P (2015) Non-destructive global and localized 2D T1/T2 NMR relaxometry to resolve microstructure in apples affected by Watercore. *Food Bioprocess Technol* 8(1):88–99. <https://doi.org/10.1007/s11947-014-1389-4>
- Melkus G, Rolletschek H, Radchuk R, Fuchs J, Rutten T, Wobus U, Altmann T, Jakob P, Borisjuk L (2009) The metabolic role of legume endosperm: a non-invasive imaging study. *Plant Physiol* 151(3):1139–1154. <https://doi.org/10.1104/pp.109.143974>
- Miki T, Saito K, Hayashi S, Kajikawa H, Shimada M, Ogawa R, Kawate Y, Ikegaya D, Kimura N, Takabatake K, Nishizawa T, Sugiura N, Suzuki M (1996) Nondestructive analysis of sugar content on watermelon using MRI device. *Teion Kogaku* 31:258–266. <https://doi.org/10.2221/jcsj.31.258>
- Mitchell J, Chandrasekera TC, Gladden LF (2012) Numerical estimation of relaxation and diffusion distributions in two dimensions. *Prog Nucl Magn Reson Spectrosc* 62:34–50. <https://doi.org/10.1016/j.pnmrs.2011.07.002>
- Mitchell J, Gladden LF, Chandrasekera TC, Fordham EJ (2014) Low-field permanent magnets for industrial process and quality control. *Prog Nucl Magn Reson Spectrosc* 76:1–60. <https://doi.org/10.1016/j.pnmrs.2013.09.001>
- Mobli M, Stern AS, Hoch JC (2006) Spectral reconstruction methods in fast NMR: reduced dimensionality, random sampling and maximum entropy. *J Magn Reson* 182(1):96–105. <https://doi.org/10.1016/j.jmr.2006.06.007>
- Munz E, Jakob PM, Borisjuk L (2016) The potential of nuclear magnetic resonance to track lipids in planta. *Biochimie* 130:97–108. <https://doi.org/10.1016/j.biochi.2016.07.014>
- Musse M, De Guio F, Quellec S, Cambert M, Challos S, Davenel A (2010) Quantification of microporosity in fruit by MRI at various magnetic fields: comparison with X-ray microtomography. *Magn Reson Imaging* 28(10):1525–1534. <https://doi.org/10.1016/j.mri.2010.06.028>
- Nestby R, Gribbestad I, Bjørgum R (1997) Magnetic resonance imaging (MRI) as a method for determination of freezing injury in strawberry crowns. *Acta Physiol Plant* 19(4):517–520. <https://doi.org/10.1007/s11738-997-0048-z>
- Pope JM, Rumpel H, Kuhn W, Walker R, Leach D, Sarafis V (1991) Applications of chemical-shift-selective NMR microscopy to the non-invasive histochemistry of plant materials. *Magn Reson Imaging* 9(3):357–363. [https://doi.org/10.1016/0730-725X\(91\)90423-J](https://doi.org/10.1016/0730-725X(91)90423-J)

- Proctor WG, Yu FC (1950) The Dependence of a Nuclear Magnetic Resonance Frequency upon Chemical Compounds. *Phys Rev* 77(5):717. <https://doi.org/10.1103/PhysRev.77.717>
- Ramsey NF (1950) A molecular beam resonance method with separated oscillating fields. *Phys Rev* 78:695–699. <https://doi.org/10.1103/PhysRev.78.695>
- Razavi MS, Asghari A, Azadbakht M, Shamsabadi HA (2018) Analyzing the pear bruised volume after static loading by magnetic resonance imaging (MRI). *Sci Hortic* 229:33–39. <https://doi.org/10.1016/j.scienta.2017.10.011>
- Redfield AG (1957) On the theory of relaxation processes. *IBM J Res Dev* 1(1):19–31. <https://doi.org/10.1147/rd.11.0019>
- Rondeau-Mouro C, Deslis S, Quellec S, Bauduin R (2015) Assessment of TD-NMR and quantitative MRI methods to investigate the apple transformation processes used in the cider-making technology. *Magn Reson Food Sci* 127–140. Capozzi F, Laghi L, Belton PS. (ed.) <https://doi.org/10.1039/9781782622741-00127>
- Saito K, Miki T, Hayashi S, Kajikawa H, Shimada M, Kawate Y, Nishizawa T, Ikegaya D, Kimura N, Takabatake K, Sugiura N, Suzuki M (1996) Application of magnetic resonance imaging to non-destructive void detection in watermelon. *Cryogenics* 36:1027–1031. [https://doi.org/10.1016/S0011-2275\(96\)00087-2](https://doi.org/10.1016/S0011-2275(96)00087-2)
- Sarafis V, Rumpel H, Pope J, Kuhn W (1990) Non-invasive histochemistry of plant materials by magnetic resonance microscopy. *Protoplasma* 159(1):70–73. <https://doi.org/10.1007/BF01326636>
- Schmidt SJ, Sun X, Litchfield JB, Eads TM (1996) Applications of magnetic resonance imaging in food science. *Crit Rev Food Sci Nutr* 36(4):357–385. <https://doi.org/10.1080/10408399609527730>
- Sersa I, Macura S (2007) Spectral resolution enhancement by chemical shift imaging. *Magn Reson Imaging* 25(2):250–258. <https://doi.org/10.1016/j.mri.2006.09.015>
- Shaw TM, Elsken RH (1956) Moisture determination, determination of water by nuclear magnetic absorption in potato and apple tissue. *J Agric Food Chem* 4:162–164. <https://doi.org/10.1021/jf60060a008>
- Solomon I (1955) Relaxation processes in a system of two spins. *Phys Rev* 99:559. <http://redeye.mmrcc.upenn.edu/mediawiki/images/d/d/A08.pdf>–565
- Sonego L, Ben-Arie R, Raynal J, Pech JC (1995) Biochemical and physical evaluation of textural characteristics of nectarines exhibiting woolly breakdown: NMR imaging, X-ray computed tomography and pectin composition. *Postharvest Biol Technol* 5(3):187–198. [https://doi.org/10.1016/0925-5214\(94\)00026-0](https://doi.org/10.1016/0925-5214(94)00026-0)
- Sozer N (ed) (2016) Imaging technologies and data processing for food engineers. Food Eng. Series. Springer International Publishing, Basel <http://www.springer.com/gp/book/9783319247335>
- Stehling MK, Turner R, Mansfield P (1991) Echo planar imaging: magnetic resonance imaging in a fraction of a second. *Science* 254(5028):43–50. <https://doi.org/10.1126/science.1925560>
- Suchanek M, Kordulska M, Olejniczak Z, Figiel H, Turek K (2017) Application of low-field MRI for quality assessment of 'Conference' pears stored under controlled atmosphere conditions. *Postharvest Biol Technol* 124:100–106. <https://doi.org/10.1016/j.postharvbio.2016.10.010>
- Sun N, Liu Y, Lee H, Weissleder R, Ham D (2009) CMOS RF biosensor utilizing nuclear magnetic resonance. *IEEE J Solid State Circuits* 44(5):1629–1643. <https://doi.org/10.1109/JSSC.2009.2017007>
- Sun T, Huang K, Xu H, Ying Y (2010) Research advances in non-destructive determination of internal quality in watermelon/melon: a review. *J Food Eng* 100(4):569–577. <https://doi.org/10.1016/j.jfoodeng.2010.05.019>
- Sun N, Yoon TJ, Lee H, Andress W, Weissleder R, Ham D (2011) Palm NMR and 1-chip NMR. *IEEE J Solid State Circuits* 46(1):342–352. <https://doi.org/10.1109/JSSC.2010.2074630>
- Szczyński PM, Strzelecki M, Materka A, Klepaczko A (2009) MaZda, a software package for image texture analysis. *Comput Methods Prog Biomed* 94(1):66–76. <https://doi.org/10.1016/j.cmpb.2008.08.005>
- Taglienti A, Ritota M, Cozzolino S, Conte L, Terlizzi M, Sequi P, Valentini M (2009) Postharvest structural changes of Hayward kiwifruit by means of magnetic resonance imaging spectroscopy. *Food Chem* 114(4):1583–1589. <https://doi.org/10.1016/j.foodchem.2008.11.066>
- Takashi M, Saito K, Hayashi S, Kogaku T (1996) Nondestructive analysis of sugar content of watermelon using MRI device. *Teion Kogaku* 31(5):258–266. <https://doi.org/10.2221/jcsj.31.258>
- Talluri S, Scheraga HA (1990) COSY with in-phase cross peaks. *J Magn Reson* 86(1):1–10. [https://doi.org/10.1016/0022-2364\(90\)90206-O](https://doi.org/10.1016/0022-2364(90)90206-O)
- Talluri S, Wagner G (1996) An optimized NOESY-HSQC. *J Magn Reson* 112(2):200–205 www.ncbi.nlm.nih.gov/pubmed/8812906
- Tse TY, Spanswick RM, Jelinski LW (1996) Quantitative evaluation of NMR and MRI methods to measure sucrose concentration in plants. *Protoplasma* 194(1–2):54–62. <https://doi.org/10.1007/BF01273167>
- Tyler DJ, Moore RJ, Marciani L, Gowland PA (2004) Rapid and accurate measurement of transverse relaxation times using a single shot multi-echo echo-planar imaging sequence. *Magn Reson Imaging* 22(7):1031–1037. <https://doi.org/10.1016/j.mri.2004.01.069>
- Utsuzawa S, Fukushima E (2017) Unilateral NMR with a barrel magnet. *J Magn Reson* 282:104–113. <https://doi.org/10.1016/j.jmr.2017.07.006>
- Vernickel P, Röschmann P, Findekle C, Lüdeke KM, Leussler CH, Overweg J, Katscher U, Grässlin I, Schünemann K (2007) Eight channel transmit/receive body MRI at 3T. *Magn Reson Med* 58(2):381–389. <https://doi.org/10.1002/mrm.21294>
- Verpillat F, Ledbetter MP, Xu S, Michalak DJ, Hilty C, Bouchard LS, Antonijevic S, Budker D, Pines A (2008) Remote detection of nuclear magnetic resonance with an anisotropic magnetoresistive sensor. *Proc Natl Acad Sci* 105(7):2271–2273. <https://doi.org/10.1073/pnas.0712129105>
- Vicente AR, Ortugno C, Rosli H, Powell ALT, Greve LC, Labavitch JM (2007) Temporal sequence of cell wall disassembly events in developing fruits. 2. Analysis of blueberry (*Vaccinium* species). *J Agric Food Chem* 55(10):4125–4130. <https://doi.org/10.1021/jf063548j>
- Wang CY, Wang PC (1989) Non-destructive detection of core breakdown in 'Bartlett' pears with nuclear magnetic resonance imaging. *Scientia Hortic* 24(1):106–109. *HortSci* 241106-109WangBartlett Pears. pdf
- Wang CY, Wang PC, Faust M (1988) Non-destructive detection of watercore in apple with nuclear magnetic resonance imaging. *Sci Hortic* 35(3–4):227–234. [https://doi.org/10.1016/0304-4238\(88\)90116-1](https://doi.org/10.1016/0304-4238(88)90116-1)
- Wilson JD (1992) Statistical approach to the solution of 1st kind integral equations arising in the study of materials and their properties. *J Mater Sci* 27(14):3911–3924. <https://doi.org/10.1007/BF00545476>
- Windt CW, Blumler P (2015) A portable NMR sensor to measure dynamic changes in the amount of water in living stems or fruit and its potential to measure sap flow. *Tree Physiol* 35(4):366–375. <https://doi.org/10.1093/treephys/tpu105>
- Winisdorffer G, Musse M, Quellec S, Devaux MF, Lahaye M, Mariette F (2015) MRI investigation of subcellular water compartmentalization and gas distribution in apples. *Magn Reson Imaging* 33(5):671–680. <https://doi.org/10.1016/j.mri.2015.02.014>
- Yoshii K, Fukuoka M, Kawamura T, Ikeda T (2013) Measuring the water status of watermelon fruits by psychrometer and ¹H nuclear magnetic resonance imaging. *Environ Control Biol* 51(3):113–120. <https://doi.org/10.2525/ecb.51.113>
- Zhang L, McCarthy MJ (2013) Assessment of pomegranate postharvest quality using nuclear magnetic resonance. *Postharvest Biol Technol* 77:59–66. <https://doi.org/10.1016/j.postharvbio.2012.11.006>
- Zhou R, Li Y (2007) Texture analysis of MR image for predicting the firmness of Huanghua pears during storage using an artificial neural

- network. *Magn Reson Imaging* 25:727–732. <https://doi.org/10.1016/j.mri.2006.09.011>
- Zhou S, Shang D, Ying Y, Liao Y (2010) Detecting subtle bruises on fruits with nuclear magnetic resonance imaging. *Nongye Jixie Xuebao/Trans Chin Soc Agric Mach* 41(8):107–110. <https://doi.org/10.3969/j.issn.1000-1298.2010.08.022>
- Zhou H, Ye ZW, Yu ZF, Su MS, Du JH (2016) Application of low-field nuclear magnetic resonance and proton magnetic resonance imaging in evaluation of ‘Jinxu’ yellow peach’s storage suitability. *Emir J Food Agric* 28(9):633–643. <https://doi.org/10.9755/ejfa.2016-03-244>
- Zion B, Chen P, McCarthy MJ (1995a) Detection of bruises in magnetic resonance images of apples. *Comp Electron Agric* 13(4):289–299. [https://doi.org/10.1016/0168-1699\(95\)00027-5](https://doi.org/10.1016/0168-1699(95)00027-5)
- Zion B, Chen P, McCarthy MJ (1995b) Non destructive quality evaluation of fresh prunes by NMR spectroscopy. *J Sci Food Agric* 67(4):423–429. <https://doi.org/10.1002/jsfa.2740670402>
- Zou X, Zhao J (eds) (2015) *Nondestructive measurement in food and agro-products*. Springer, Rotterdam. <https://doi.org/10.1007/978-94-017-9676-7>
- Zur N, Shlizerman L, Ben-Ari G, Sadka A (2017) Use of magnetic resonance imaging (MRI) to study and predict fruit splitting in citrus. *Hortic J* 86(2):151–158. <https://doi.org/10.2503/hortj.MI-147>